

## MOVPE GaN/AlGa<sub>N</sub> HEMT NANO-STRUCTURES

<sup>1</sup>Eduard HULICIUS, <sup>1</sup>Karla KULDOVÁ, <sup>1</sup>Alice HOSPODKOVÁ, <sup>1</sup>Jiří PANGRÁC, <sup>1</sup>Filip DOMINEC,  
<sup>2</sup>Josef HUMLÍČEK, <sup>1</sup>Ivan PELANT, <sup>1</sup>Ondřej CIBULKA, <sup>1</sup>Kateřina HERYNKOVÁ

<sup>1</sup>*Institute of Physics of the CAS, Prague, Czech Republic, EU, [hulicius@fzu.cz](mailto:hulicius@fzu.cz)*

<sup>2</sup>*Masaryk University, Central European Institute of Technology, Brno, Czech Republic, EU*

### Abstract

GaN/AlGa<sub>N</sub>-based high electron mobility transistors (HEMTs) attain better performance than their state-of-the-art full silicon-based counterparts, offering higher power, higher frequency as well as higher temperature of operation and stability, although their voltage and current limits are somewhat lower than for the SiC-based HEMTs. GaN/AlGa<sub>N</sub>-based HEMTs are a potential choice for electric-powered vehicles, for which they are approved not only for their power parameters, but also for their good temperature stability, lifetime and reliability. It is important to optimize HEMT structures and their growth parameters to reach the optimum function for the real-world applications.

HEMT structures described and discussed here were grown by MOVPE technology in AIXTRON apparatus on (111)-oriented single-surface polished 6" Si substrates.

Structural, optical and transport properties of the structures were measured by X-ray diffraction, optical reflectivity, time-resolved photoluminescence and  $\mu$ -Raman spectroscopy.

**Keywords:** HEMT, MOVPE, nitrides, quantum well

### 1. INTRODUCTION

There are many approaches how to prepare HEMT structures which can be used for many potential application namely for electric-powered vehicles, for which they are approved not only for their power parameters, but also for their good temperature stability, lifetime and reliability. GaN can be the semiconductor of choice for power converters throughout vehicle electronics with devices capable of switching as much as 100 A at 900 V.

Silicon-based insulated gate bipolar transistors (IGBTs), superjunction MOSFETs and HEMTs are fundamental components of current power electronic systems for the conversion, control and conditioning of electrical energy. If silicon devices were to be replaced by a more efficient semiconductor such as GaN, compact converters with ultra-high density could be designed only because the breakdown strength and electron mobility in GaN are much higher [1,2]. GaN based HEMTs are very hot topic. There are about 5 000 papers at Web of Science and more than 50 review articles. We can recommend topical review "The 2018 GaN power electronics roadmap" [3] and the literature cited there. Industrial companies (eg. Transphorm, EPC, Panasonic, Infineon, GaN Systems, Dialog and Navitas) made much investments of a wide variety of markets exploring the use of the technology in new circuit topologies, packaging solutions and system architectures that are required to achieve and optimize the system advantages offered by GaN transistors, nevertheless it is important to optimize HEMT structures and their growth parameters to reach the optimum function for the real-world applications. A small part of this effort is presented in the article [3].

### 2. EXPERIMENTAL

MetalOrganic Vapor Phase Epitaxy (MOVPE) is the leading technology currently; Molecular Beam Epitaxy (MBE) covers only few percent of structure growing, mainly for the research.

GaN cap	1-2 nm
Al <sub>0.24</sub> Ga <sub>0.76</sub> N barrier	19 nm
AlN spacer	1 nm
u-GaN	0.2 μm
GaN:C (~1E19cm <sup>-3</sup> )	2.0 μm
u-GaN	0.6 μm
Al <sub>0.25</sub> Ga <sub>0.75</sub> N	450 nm
Al <sub>0.45</sub> Ga <sub>0.55</sub> N	250 nm
Al <sub>0.60</sub> Ga <sub>0.40</sub> N	200 nm
AlN	~200 nm
Si (111)	1150 μm

**Figure 1** HEMT structure No. 6516 grown on 1.15 mm thick Si substrates with diameter of 200 mm

The structure No. 6516 presented in this article was grown with MOVPE AIXTRON apparatus on (111)-oriented single-surface polished 8" Si substrates. GaN/AlGaN structure is shown in **Figure 1**.

The second structure No. 6508 used in 2.1.2. and 2.1.4. sections as a reference sample was grown on (111)-oriented single-surface polished 6" Si substrates with slightly different Al and Ga composition in the AlGaN layers (see **Figure 8**).

Room-temperature time resolved photoluminescence (TR-PL) was excited by the four harmonic wavelength of a femtosecond laser Pharos (257 nm, 4.8 eV) with pulse duration of 160 fs, energy 17 μJ and repetition rate of 1 kHz. PL detection was carried out by a Hamamatsu streak camera.

Raman and steady-state photoluminescence (PL) spectra were measured at RT using LabRAM HR Evolution Raman microscope in backscattering configuration. The PL spectra were excited with a 325 nm laser line and the Raman spectra with a 532 nm line, both with a circular spot of about 1 μm in diameter. The signal was collected from the top of the wafer in z(y,-)z configuration in Porto's notation. The Raman measurements were performed with spectral resolution better than 1 cm<sup>-1</sup>.

## 2.1. Measurements and discussion

### 2.1.1. X-ray diffraction measurement

The sample exhibits rather good crystallographic quality, as can be seen in **Figure 2**.

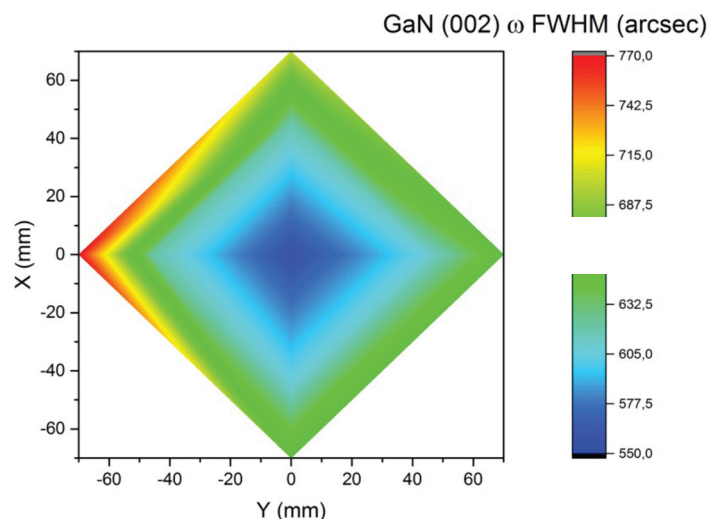


**Figure 2** X-ray diffraction measured of GaN (002) ω FWHM - 9 points cross-map. GaN (102) ω FWHM in center point = 1234 arcsec

### 2.1.2. Optical reflectivity

Reflectivity of two different HEMT structures and a bare Si substrate was measured from 1.2 to 5.1 eV - see **Figure 3**. The lateral homogeneity of the wafers was tested by taking the spectra at several positions, the

diameter of the circular measurement area being about 1 mm. Interference (Fabry-Perot-like) pattern below the gap of GaN (~3.4 eV) is due to the coherent reflections in the buffer and channel layers. Above ~3.5 eV, the spectra show reflectivity of the opaque GaN channel layer, modified by the presence of a thin AlGaN barrier layer. The latter leads to pronounced spectral changes around the energy of the (exciton) bandgap, moving to higher photon energies with increasing Al content (the arrows in **Figure 3**).

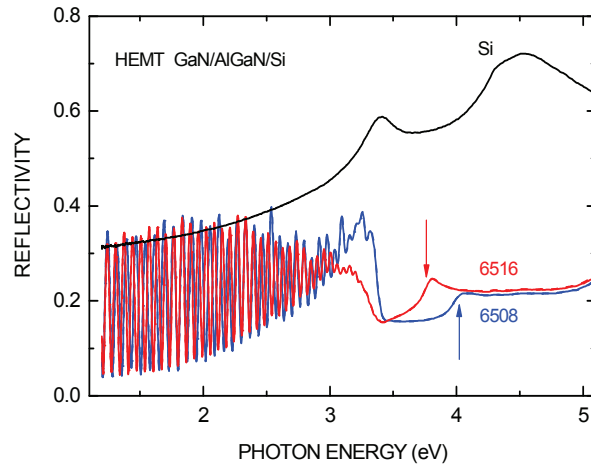


**Figure 3** Reflectivity of two HEMT samples 6516 and 6508, measured at their center and 1 cm off center - red and blue colors

A closer look at the spectral positions, using the second derivatives of the reflectance in order to localize the transition energies, leads the Al contents of 15 and 22 at. % for the 6516 and 6508 samples, respectively. These estimates are rather different from the nominal values of 24 and 25 at. % Al.

### 2.1.3. Steady-state photoluminescence

The micro-PL spectra excited with three different intensities of 325 nm line are presented in **Figure 4**. We can distinguish in these spectra three maxima: the first one at 360 nm is due to emission of GaN exciton, the second one between 500 nm and 720 nm is the well-known yellow band (YB) of GaN defects and, between them, a low intensity emission from 400 nm to 500 nm corresponding to unidentified defects which are still under discussion. The spectra are normalized to the exciton peak intensity, and strong saturation of the YB for higher excitation intensities is evident.

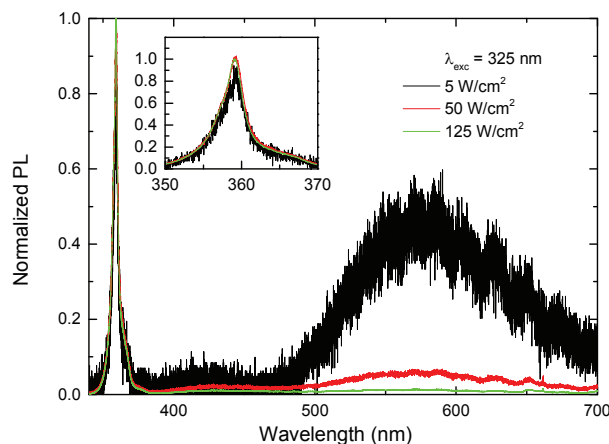


**Figure 4** Comparison of PL spectra normalized to exciton peak intensity excited by three different excitation intensities. Relative contribution of YB luminescence is decreasing with excitation intensity due to a long decay time and saturation of this maximum

### 2.1.4. Time resolved photoluminescence

TR-PL and PL decay time at 555 nm of the GaN YB measured at our HEMT sample are shown in **Figure 5**. This emission band is modulated due to the interferences in some of thin layers, most probably that of GaN 400 nm thick. Decay time for 1/e of intensity is 34  $\mu$ s.

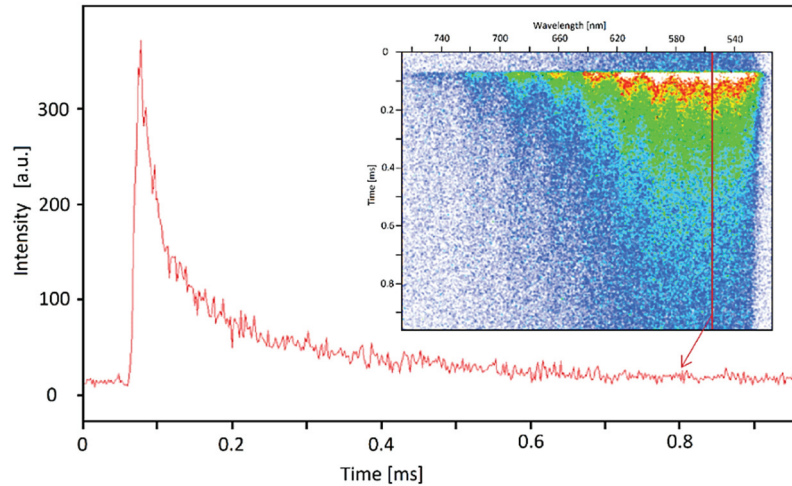


**Figure 5** PL decay at 555 nm: decay time (1/e) = 34  $\mu$ s. Insert: Two-dimensional map of TR-PL of the complete YB at 520-760 nm

Rather fast TR-PL emissions at around 360 nm (3.44 eV) - probably from the 400 nm thick GaN layer -, and at 315 nm (3.93 eV) - probably exciton from a 25 nm thick AlGaIn barrier, are shown in **Figure 6**. The sample was excited as described above, only the repetition frequency was of 3 kHz. Detection was carried out again by the Hamamatsu streak camera; notice, however, that the time scale here is by 6 orders of magnitude faster.

The PL peak at 315 nm (3.93 eV) cannot be excited by the 325 nm laser, but its spectral position is probably indicated in the reflectivity spectrum at around 3.8-4.0 eV - see **Figure 3**. PL dynamic properties of this weak peak are shown in **Figure 6**. Decay time is expected to be faster than the measured 22 ps because deconvolution of the excitation pulse was not executed.

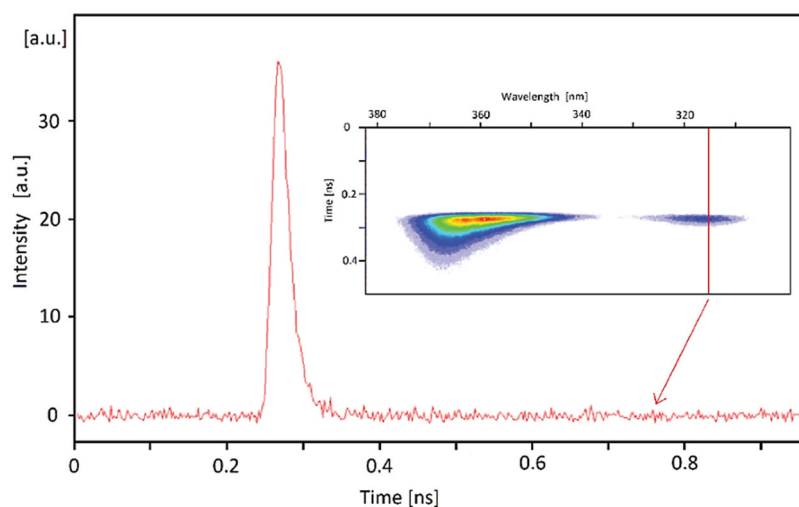


**Figure 6** TR-PL of AlGaIn emission at 315 nm, decay time (1/e) = 22 ps, dynamic of PL is much faster than for YB. Insert: Two-dimensional map of TR-PL of the GaN and AlGaIn emission, the spectral line of AlGaIn emission at 315 nm has FWHM of 14 nm

TR-PL of the GaN emission at around 360 nm is shown in **Figure 7**. Dynamic properties of PL are much faster than for the YB, decay times are again in the order of ten ps.

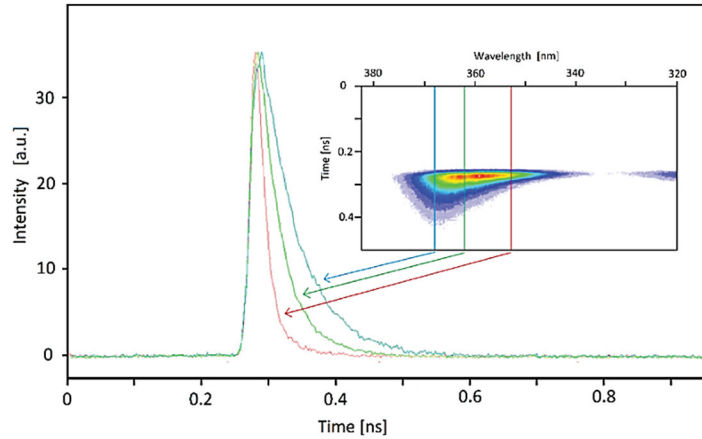


**Figure 7** PL decay of GaN emission at 353, 362 and 368 nm: decay times (1/e) = 20, 38 and 56 ps, resp. Insert: Map of time resolved GaN PL, the spectral FWHM of the line is about 17 nm

### 2.1.5. Micro-Raman spectra

In Raman spectroscopy, we focused on the longitudinal optical mode A1(LO) because it is sensitive to Al composition in  $\text{Al}_x\text{Ga}_{1-x}\text{N}$  heterostructure but rather insensitive to strain [4]. The A1(LO) mode exhibits a single-mode behavior and its energy in  $\text{Al}_x\text{Ga}_{1-x}\text{N}$  as a function of  $x$  was several times refined by various authors. We have used the calibration curve for the A1(LO) phonon mode from [4].

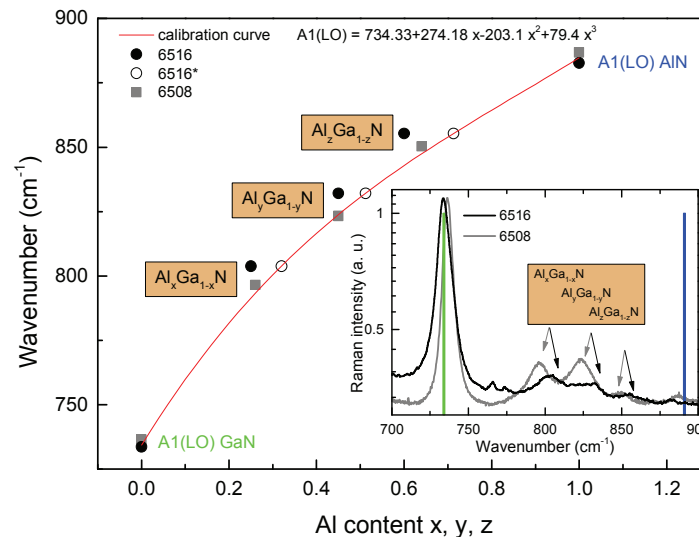


**Figure 8** Calibration curve (red line) equation is taken from [4]. Insert shows Raman spectra of samples No. 6516 and 6508. The reference sample No. 6508 has  $x = 0.26$ ,  $y = 0.45$  and  $z = 0.64$

Shown in the insert of the **Figure 8** are Raman spectra of sample No. 6516 and reference sample No. 6508 in the spectral region between A1(LO) mode of GaN and that of AlN. Green and blue lines mark their spectral positions in bulk materials, respectively. Between this two positions, one can see three small peaks corresponding to three  $\text{Al}_x\text{Ga}_{1-x}\text{N}$  layers with Al composition  $x = 0.25$ ,  $y = 0.45$  and  $z = 0.60$ ;  $x = 0.26$ ,  $y = 0.45$  and  $z = 0.64$  for the reference sample. Raman signal from a thin  $\text{Al}_m\text{Ga}_{1-m}\text{N}$  layer under the GaN cap with  $m =$

0.24 (6516) or  $m = 0.25$  (6508) of Al composition cannot be distinguished from the first thick  $\text{Al}_x\text{Ga}_{1-x}\text{N}$  layer with  $x = 0.25$  (6516) or 0.26 (6508).

Positions of maxima of all peaks corresponding to A1(LO) mode frequencies are shown by full symbols in **Figure 8**.

As we can see, the positions of the A1(LO) peak of heterostructure layers of the reference sample are in good agreement with the values of the calibration curve. This is no more true for the sample No. 6516. There is a systematic shift towards a lower composition of Al in the structure. The composition values corresponding better to the measured frequencies, according to the calibration curve, are marked by open circles. The values of Al composition corresponding to those points are  $x = 0.30$ ,  $y = 0.50$  and  $z = 0.70$ .

### 3. CONCLUSIONS

GaN/AlGa<sub>N</sub> HEMT structures were prepared by MOVPE. X-ray diffraction measurement shows a good crystallographic quality of the structure.

Reflectivity measurement was used to establish thickness and Al composition. Measurements at different positions show good structure homogeneity.

PL, and especially TR-PL, have proved suitable tools for structure speed response and defect type and composition estimation.

Al composition in  $\text{Al}_x\text{Ga}_{1-x}\text{N}$  heterostructure as measured by Raman spectroscopy supplies feedback for grower intentions and aims.

### ACKNOWLEDGEMENTS

*Authors acknowledge support from the Technology Agency of the Czech Republic, project No. TH02010014 and MSMT NPU project no. LO1603 - ASTRANIT.*

### REFERENCES

- [1] YANG, L., CHENG, C.W., BULSARA, M.T. and FITZGERALD, E.A., High mobility  $\text{In}_{0.53}\text{Ga}_{0.47}\text{As}$  quantum-well metal oxide semiconductor field effect transistor structures. *J. Appl. Phys.* 2012. vol. 111, 104511.
- [2] BRENNAN, B., ZHERNOKLETOV, D.M., DONG, H., HINKLE, C.L., KIM, J. and WALLACE, R.M., In situ surface pre-treatment study of GaAs and  $\text{In}_{0.53}\text{Ga}_{0.47}\text{As}$ . *Appl. Phys. Lett.* 2012. vol. 100, 151603.
- [3] AMANO H., BAINES Y., BEAM E., et al, The 2018 GaN power electronics roadmap. *J. Phys. D: Appl. Phys.* 2018. vol. 51, 163001.
- [4] WANG, Ch., CAHA, O., MUNZ, F., KOSTELNÍK, P., NOVÁK, T. and HUMLÍČEK, J., Mid-infrared ellipsometry, Raman and X-ray diffraction studies of  $\text{Al}_x\text{Ga}_{1-x}\text{N}/\text{AlN}/\text{Si}$  structures. *Applied Surf. Sci.* 2017. vol. 421, 859-865.